TABLE I
CAPACITANCE PARAMETERS EXTRACTED WITH BOTH APPROACHES UNDER CONSIDERATION

Parameter	Generally used method	Newly developped method
C_{gs0}	682.6 fF	621.4 fF
C_{gd0}	33.4 fF	32.1 fF
V_{bi}	1.92 V	0.921 V

satisfied. Setting a large gate–drain voltage guarantees that the term $(V_{\rm gs}-V_{\rm gd})^2$ in (2) is large compared to α^{-2}, and the assumption of a large α is valid. Under these conditions, $V_{\rm new}$ is negligible in (1) and $K_1 = 1$ and $K_2 = 1$. The capacitance equations then reduce to (8)

$$C_{\rm gs} = C_{\rm gs0}$$
$$C_{\rm gd} = C_{\rm gd0}. \tag{8}$$

Evidence for (8) can also be found on simulated characteristics (Figs. 2 and 3, since $V_{\rm gs}$ is nearly zero, large $(V_{\rm gs} - V_{\rm gd})^2$ is equivalent to large $V_{\rm ds}$). It has been demonstrated that the parameters wanted to be extracted can be calculated easily from measured S-parameters for one particular bias point. All necessary optimizations need only be performed for a single bias point. In addition, the influence of the (earlier extracted) α-parameter and $V_{\rm bi}$ were eliminated. The value of $V_{\rm bi}$ can be easily determined from measurements at one additional bias point.

III. MEASUREMENTS

The modeled parameter extraction was first tested on modeled data. In that case, both approaches under consideration work almost equally well. However, when the extraction was performed on a real device, an important discrepancy between measured S-parameters and those simulated with parameters extracted using the generally used routine (Figs. 4 and 5) was observed. The device used was a 6×100 μm GaAs MESFET with a 0.7-μm gate length. The DC-parameters [7] and parasitics [8], [9] were extracted with established extraction procedures. The extracted capacitance parameters are listed in Table I. To accentuate the discrepancy, a comparison is shown (in Figs. 4 and 5) between measurement and simulation of the real part of S_{12} where the new method performs best, and the imaginary part of S_{11}, where it performs worst (but still better than the generally used method). Figs. 4 and 5 also indicate two striking features of simulation results obtained with the new method. First, a significant reduction in the error magnitude is achieved and also a better correspondence between the shapes of measured and simulated curves is obtained. The reason for these large differences for the measured results, in comparison with the extraction on modeled data, lies in the contribution of errors introduced by the influence of $V_{\rm bi}$ on the extraction procedure. It is clear that this new method is far less sensitive to these errors.

IV. CONCLUSION

A new, fast, and reliable method for the extraction of the nonlinear Statz-MESFET-model capacitance parameters was developed. The method gives good simulation results, both on real and modeled data. This method is far more robust and insensitive to measurement errors than the formerly used one because the number of parameters to be simultaneously extracted was reduced from three to two, which eliminated the influence of earlier extracted parameters such as α. The mutual influence of $C_{\rm gs0}$ and $C_{\rm gd0}$ was also eliminated.

REFERENCES

[1] W. R. Curice, "A MESFET model for use in the design of GaAs circuits," *IEEE Trans. Microwave Theory Tech.*, vol. MTT-28, pp. 448–456, May 1980.

[2] H. Statz, P. Newman, I. W. Smith, R. A. Pucel, and H. A. Haus, "GaAs FET device and circuit simulation in SPICE," *IEEE Trans. Electron Devices*, vol. ED-34, pp. 160–169, Feb. 1987.

[3] D. Divekar, "Comments on 'GaAs FET device and circuit simulation in SPICE,'" *IEEE Trans. Electron Devices*, vol. ED-34, pp. 2564–2565, Dec. 1987.

[4] I. W. Smith, H. Statz, H. A. Haus, and R. A. Pucel, "On charge nonconservation in FET's," *IEEE Trans. Electron Devices*, vol. ED-34, pp. 2565–2568, Dec. 1987.

[5] J. Rodriguez-Tellez, K. Mezher, and M. Al-Daas, "Computationally efficient and accurate capacitance model for the GaAs MESFET for microwave nonlinear circuit design," *IEEE Trans. Computer-Aided Design*, vol. 13, pp. 1489–1497, Dec. 1994.

[6] V. I. Cojocaru and T. J. Brazil, "Modeling the gate capacitances of MESFET's and HEMT's from low-frequency C–V measurements," in *23rd European Microwave Conf. Proc.*, Madrid, Spain, Sept. 1993, pp. 511–513.

[7] J. M. Golio, *Microwave MESFET's and HEMT's.* Norwood, MA: Artech House, 1991.

[8] P. Debie and L. Martens, "Fast and accurate extraction of parasitic resistances for nonlinear GaAs MESFET device models," *IEEE Trans. Electron Devices*, vol. 42, pp. 2239–2242, Dec. 1995.

[9] J. C. Costa, M. Miller, M. Golio, and G. Norris, "Fast, accurate, on-wafer extraction of parasitic resistances and inductances in GaAs MESFET's and HEMT's," in *IEEE MTT-S Int. Microwave Symp. Dig.*, Albuquerque, NM, June 1992, pp. 1011–1014.

A Novel Ultrawideband Microwave Differential Phase Shifter

F. V. Minnaar, J. C. Coetzee, and J. Joubert

***Abstract*—Wideband microwave phase shifters are usually constructed using cascaded coupled-line sections connected together at their far ends. By utilizing the unique frequency-independent quadrature property of symmetric couplers, a new class of phase shifter is proposed. The use of ultrawideband couplers in its realization results in a device which offers greater freedom with respect to bandwidth and ripple. The tendency of symmetrical networks to cancel small errors due to manufacturing tolerances is also exploited in order to improve its high-frequency performance.**

***Index Terms*— Microwave phase shifter, stripline components, wideband.**

I. INTRODUCTION

Differential phase shifters find wide application in microwave systems, for example, in hybrid circuits and wideband phased-array antennas. They are three-port or four-port networks providing a

Manuscript received August 23, 1996; revised April 25, 1997.

The authors are with the Department Electrical and Electronic Engineering, University of Pretoria, Pretoria 0002, South Africa.

Publisher Item Identifier S 0018-9480(97)05382-9.

constant differential phase shift across their two output ports. For wideband applications, these devices are almost exclusively realized in stripline, due to its nondispersive and broadband propagation properties.

The basic Schiffman phase shifter [1] consists of two separate TEM transmission lines, one of which is a C-section consisting of a pair of coupled lines directly connected to each other at one end. The other line is a length of uncoupled line, denoted as the reference line. It introduces a phase shift linearly dependent on the frequency with respect to the input signal, while a differential phase shift between the output ports of the C-section and the reference line is established. The coupled section is one-quarter wavelength long at the center frequency. Schiffman identified six different configurations employing coupled-line sections [1], and later extended the design procedure to cover wideband multisection phase shifters consisting of a cascade of pairs of coupled transmission lines connected together at their far ends [2]. Schiffman concluded that a $5:1$ bandwidth may be covered using these networks. Tresselt published a design procedure for a continuously tapered coupled-section phase shifter [3]. He realized the important fact that the spread in coupling values between adjacent sections is large enough to produce significant reactive discontinuities in practical TEM line geometries, which adversely affects the VSWR and phase accuracy of stepped devices at high frequency. His continuously tapered synthesis procedure considerably reduced the impact of these effects. He designed and constructed such a device over a $10:1$ band. However, the results showed that the interconnecting strap parasitics limited the upper frequency band and could only be partially compensated for, limiting the device application to about 9 GHz. Meschanov *et al.* [4] proposed a structure consisting of a cascade of coupled-line pairs of varying length and coupling coefficients and each connected together at one end. They used an optimization technique to calculate the parameters of the different sections. Apart from this contribution, virtually all work regarding wideband differential phase shifters was based on Schiffman's original work, and involved improvements or extensions to the classical Schiffman phase shifter, the most recent being an accurate analysis of microstrip phase shifters [5].

In this paper, a new class of differential phase shifters is proposed. It utilizes the unique property of frequency-independent quadrature split for symmetrical directional couplers. By connecting ultrawideband couplers in a unique configuration, an ultrawideband differential phase shifter is constructed. As in [3], the band-limiting factors are physical transitions and etching tolerances, but by utilizing the concept of symmetry, these effects are alleviated. This extends the upper frequency limit appreciably. This new class of microwave differential phase shifters offers superior performance with respect to bandwidth, upper frequency limit, size, and synthesis effort.

II. Principle of Operation

The coupling factor k of a directional coupler specifies the voltage ratio of coupled versus incident power for a coupler. A single-section coupler achieves this coupling coefficient only over a limited frequency band. However, by increasing the number of sections, the bandwidth may be increased significantly. The number of sections required and their coupling values depend on the bandwidth and ripple specification. Equal-ripple Chebyshev multisection-coupler design tables covering up to $20:1$ bandwidths have been tabulated by Crystal and Young [6]. Very high isolation and realizability into the mm-band can be achieved in stripline, using the nonuniform tapered-line synthesis techniques of Tresselt [7]. This tapered-line realization avoids transitional parasitics due to higher mode excitation at section discontinuities. For stripline couplers, the maximum achievable coupling is limited. However, by connecting couplers in tandem, any level can be achieved without compromising bandwidth or ripple.

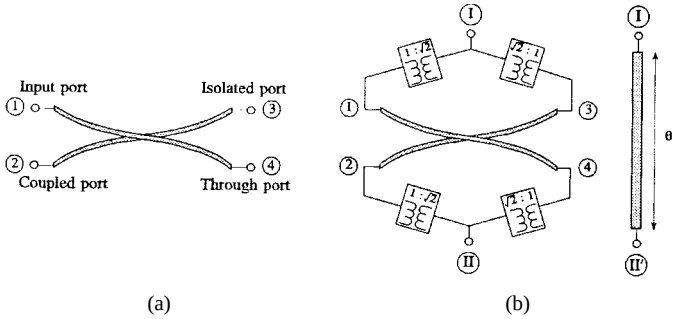

Fig. 1. (a) Symmetrical ultrawideband coupler realized as broadside-coupled striplines. (b) Configuration of an ultrawideband differential phase shifter.

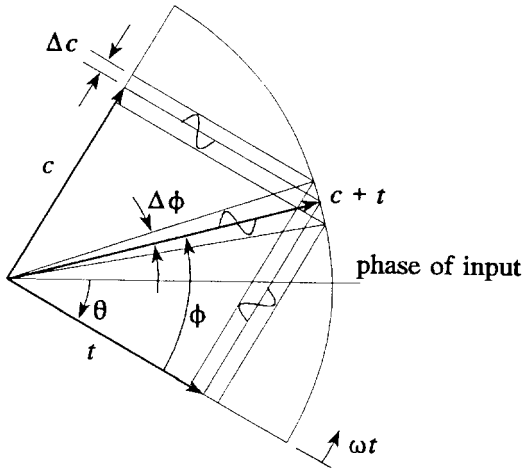

Fig. 2. Phasor representation of phase-shifter action.

For the multisection symmetrical coupler shown in Fig. 1(a), the output coupling and transmission coefficients are, in general, given by

$$\begin{aligned} c &= jke^{-j\theta} \\ t &= \sqrt{1-k^2}e^{-j\theta} \end{aligned} \tag{1}$$

where $k = k(\omega)$ is an equi-ripple coupling function over the design bandwidth, while $\theta = \theta(\omega)$ is a phase term linearly dependent on frequency, taken as the electrical length of the through path. It is clear that c always leads t by 90°, independent of frequency. This is a property unique to all symmetrical directional couplers [6]–[8]. The scattering parameters of an ideal coupler are then defined in terms of these coefficients [8]. Using the general definition for S-parameters, one obtains

$$\begin{bmatrix} b_1 \\ b_2 \\ b_3 \\ b_4 \end{bmatrix} = \begin{bmatrix} 0 & c & 0 & t \\ c & 0 & t & 0 \\ 0 & t & 0 & c \\ t & 0 & c & 0 \end{bmatrix} \begin{bmatrix} a_1 \\ a_2 \\ a_3 \\ a_4 \end{bmatrix}. \tag{2}$$

By connecting the coupled port and transmission port through $\sqrt{2}:1$ voltage transformers, and similarly applying the input signal to both the input port and isolation port, the phase shifter depicted in Fig. 1(b) results. If one accordingly sets $a_1 = a_3 = a_{\mathrm{I}}/\sqrt{2}$ and $a_2 = a_4 = 0$ in (2), one finds that

$$\begin{aligned} b_2 = b_4 &= \frac{b_{\mathrm{II}}}{\sqrt{2}} = (c+t)\frac{a_{\mathrm{I}}}{\sqrt{2}} \\ b_1 = b_3 &= b_{\mathrm{I}} = 0. \end{aligned} \tag{3}$$

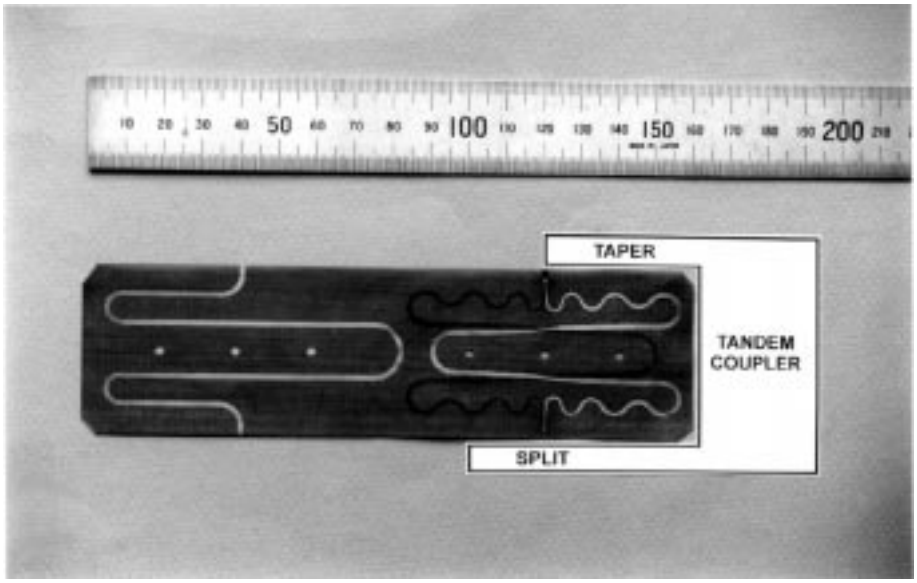

Fig. 3. Photograph of the center substrate of the manufactured prototype.

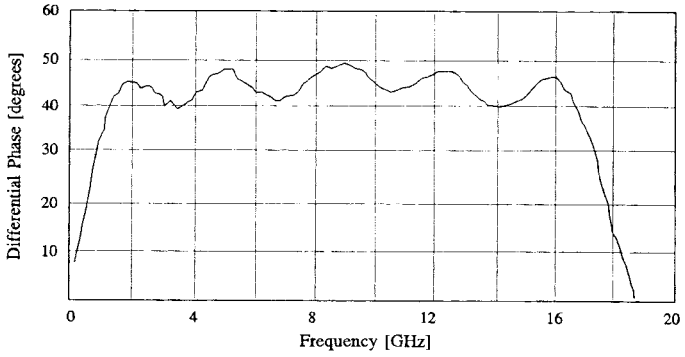

Fig. 4. Measured phase response for a 1–18-GHz phase shifter.

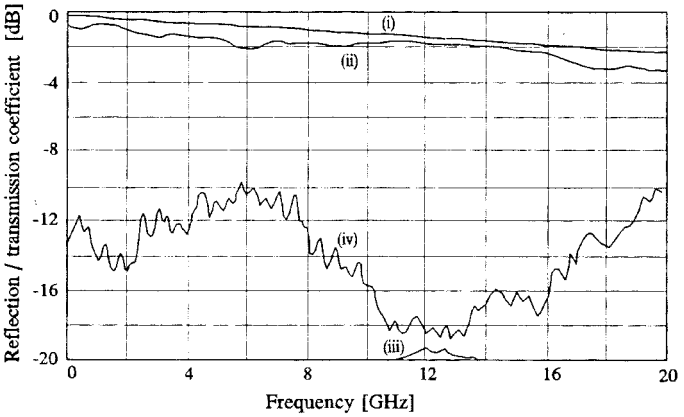

Fig. 5. Measured data for the transmission coefficient of (i) the reference line and (ii) the phase shifter, as well as the reflection coefficient of the (iii) reference line and (iv) phase shifter.

A transform defined by $k = \sin(\phi)$ is introduced, where k is the frequency-dependent coupling coefficient and ϕ is the frequency-dependent coupling angle. Thus, (3) yields

$$b_{\rm II} = a_{\rm I}(c + t) = a_{\rm I}(\cos\phi + j\sin\phi)e^{-j\theta} = a_{\rm I}e^{j\phi}e^{-j\theta}. \quad (4)$$

If the same input is applied to the reference line, one obtains that

$$b_{\rm II'} = a_{\rm I}e^{-j\theta}. \quad (5)$$

Thus, the circuit provides a phase shift ϕ, relative to the phase of the reference line over the device bandwidth, since

$$b_{\rm II} = b_{\rm II'}e^{j\phi}. \quad (6)$$

Due to the ripple in the value of k, the phase shift ϕ also displays a ripple as illustrated in Fig. 2. For the case of the circuit in Fig. 1(b), θ includes the electrical length of two split arms as well. Note that, theoretically, there is no energy loss. The same result could have been obtained without connecting the input to the isolated port as well, but the configuration of Fig. 1(b) results in a symmetrical network. The tendency of symmetrical networks to cancel small errors due to manufacturing tolerances is thus exploited in order to improve the high-frequency operation.

For a required phase shift ϕ_0, the nominal coupling coefficient of the coupler is obtained from

$$C_0 = 20\log[\sin(\phi_0)] \text{ dB} \quad (7)$$

while the phase shift ripple $\Delta\phi$ is related to the coupling ripple, ΔC, via

$$\Delta C = 20\log\left[\frac{\sin(\phi_0 + \Delta\phi)}{\sin(\phi_0)}\right] \text{ dB}. \quad (8)$$

If the required coupling coefficient is so tight as to necessitate the use of N couplers in tandem, the parameters of the individual sections are obtained by setting $\phi_0 = \sum_{n=1}^{N}\phi_{0n}$ and $\Delta\phi = \sum_{n=1}^{N}\Delta\phi_n$, and calculating the nominal coupling coefficient C_{0n} and ripple-level ΔC_n of the nth coupler using (7) and (8).

III. Example

In order to demonstrate the principles, a $45^\circ \pm 5^\circ$ phase shifter over a 1–18 GHz frequency band was synthesized. This required a coupler with a nominal coupling coefficient of $C_0 = -3.01$ dB and a maximum ripple of $\Delta C = 0.695$ dB. It was decided to connect two couplers in tandem, each with a nominal coupling coefficient of -8.343 dB and a ripple level of 0.862 dB. The coupler design was based on a nine-section structure, of which the parameters were obtained from [6], after which the continuously tapered synthesis

procedure of [7] was applied to alleviate the problems associated with the reactive discontinuities at section junctions. The couplers were constructed employing offset parallel-coupled striplines, with the line dimensions obtained from [9]. The tri-plate stripline structure consisted of two Duroid RT/5880 substrates of 31-mil thickness and relative permittivity 2.2, with a similar substrate of 5-mil thickness sandwiched between them. The transformers shown in Fig. 1(b) were implemented as 100–50-Ω impedance tapers, thereby matching the split to the 50-Ω coupler, and again to combine the two coupler output signals. Fig. 3 shows a photograph of the center substrate of the manufactured prototype, with the reference line on the left-hand side, and the phase shifter toward the right. The symmetrical phase shifter produced satisfactory results over a bandwidth of 1–17 GHz, as shown in Fig. 4. The results confirm the theory, but practical difficulties with especially the implementation of the splits were experienced. These were constructed using a number of via connections, and the resulting asymmetry deteriorated the high-frequency performance. Measured results for the reflection and transmission coefficients shown in Fig. 5 were also satisfactory. The insertion loss exceeds 3 dB at the higher end of the frequency range, but this may largely be attributed to inherent losses, as seen from the result shown for the reference line. Only a small portion of the curve for the reflection coefficient of the reference line is visible, since it is below -20 dB for nearly the whole frequency range.

A 90° phase shifter can be constructed by either cascading two 45° phase shifters, or by directly applying the synthesis technique. The latter will require a coupler with a nominal coupling coefficient of 0 dB, which may be realized by means of a tandem connection of two -3.01-dB couplers, or in practice, four -8.343-dB couplers. Employing couplers identical to those used in the previous example (i.e., $C_{0n} = -8.343$ dB and $\Delta C_n = 0.862$ dB) will result in a differential phase shift of $90° \pm 10°$. The insertion loss will ideally still be zero. However, due to the additional line length, the total dielectric and ohmic losses are expected to almost double in comparison to those of the 45° phase shifter. Applications where the input signal is to be simultaneously applied to both the input ports of a 90° phase shifter and the reference line will require the use of a power splitter. For these applications, a better option will be to merely use a symmetrical wideband -3.01-dB coupler as shown in Fig. 1(a), where a differential phase shift of 90° and negligible phase ripple between the signals at the coupled and through ports are established intrinsically.

IV. Conclusion

Progress in the field of wideband microwave has largely been limited to improvements or extensions to one of the six basic classes of Schiffman phase shifters, thereby restricting the realizability of these devices to about 9 : 1 bandwidth, up to 12 GHz. The novel class of ultrawideband phase shifters proposed here has the possibility of achieving up to a 20 : 1 bandwidth, extended to an upper limit of 20 GHz. Practical results confirmed the theory, although certain aspects like the implementation of the split to the coupler still need to be refined.

Acknowledgment

The authors acknowledge, with gratitude, the support of Grinaker Avitronics during the course of this research.

References

[1] B. M. Schiffman, "A new class of broad-band microwave 90° phase shifters," *IRE Trans. Microwave Theory Tech.*, vol. MTT-6, pp. 232–237, Apr. 1958.
[2] ——, "Multisection microwave phase shift network," *IEEE Trans. Microwave Theory Tech.*, vol. MTT-14, pp. 209, Apr. 1966.
[3] C. P. Tresselt, "Broad-band tapered-line phase shift networks," *IEEE Trans. Microwave Theory Tech.*, vol. MTT-16, pp. 51–52, Jan. 1968.
[4] V. P. Meschanov, I. V. Metelnikova, V. D. Tupikin, and G. G. Chumaevskaya, "A new structure of microwave differential phase shifter," *IEEE Trans. Microwave Theory Tech.*, vol. 42, pp. 762–765, May 1994.
[5] C. E. Free and C. S. Aitchison, "Improved analysis and design of coupled-line phase shifters," *IEEE Trans. Microwave Theory Tech.*, vol. 43, pp. 2126–2131, Sept. 1995.
[6] E. G. Crystal and L. Young, "Theory and tables of optimum symmetrical TEM-mode coupled-transmission-line directional couplers," *IEEE Trans. Microwave Theory Tech.*, vol. MTT-13, pp. 544–558, Sept. 1965.
[7] C. P. Tresselt, "The design and construction of broad-band high-directivity, 90° couplers using nonuniform line techniques," *IEEE Trans. Microwave Theory Tech.*, vol. MTT-14, pp. 647–656, Dec. 1966.
[8] J. A. G. Malherbe, *Microwave Transmission Line Couplers*. Norwood, MA: Artech House, 1988.
[9] J. P. Shelton, "Impedances of offset parallel-coupled strip transmission lines," *IEEE Trans. Microwave Theory Tech.*, vol. 14, pp. 7–15, Jan. 1966.

A Simple and Accurate MESFET Channel-Current Model Including Bias-Dependent Dispersion and Thermal Phenomena

Tae Moon Roh, Youngsik Kim, Youngsuk Suh, Wee Sang Park, and Bumman Kim

***Abstract*— A new channel-current model of GaAs MESFET suitable for applications to microwave computer-aided design (CAD) has been developed. This model includes the frequency-dispersion effects due to traps and thermal effects. The model parameters are extracted from pulsed *I–V* measurements at several ambient temperature and quiescent bias points. This model is verified by simulating nonlinear circuits, such as a power amplifier and a mixer.**

I. Introduction

For microwave-circuit design, commercially available computer-aided design (CAD) software is widely used. These CAD tools are based on the accurate device models, and a proper modeling is very important. In large-signal modeling, the gate–source and drain–source voltage-controlled drain–source channel current $I_{\rm ds}(v_{\rm gs}, v_{\rm ds})$ is the most important element because it is the major nonlinear component. The usual measurement method for determining $I_{\rm ds}(v_{\rm gs}, v_{\rm ds})$ is pulsed *I–V* technique [1]-[5], which is free from the frequency dispersion due to deep-level trap/surface state and thermal

Manuscript received November 5, 1996; revised April 25, 1997. This work was supported in part by the Agency for Defense Development.

T. M. Roh, Y. Kim, W. S. Park, and B. Kim are with the Department of Electronic and Electrical Engineering and Microwave Application Research Center, Pohang University of Science and Technology, Pohang, Kyung-pook, 790-784, Korea.

Y. Suh is with the School of Electrical and Electronic Engineering Yeungnam University, Gyongsan, Kyungbuk, 712-749, Korea.

Publisher Item Identifier S 0018-9480(97)05383-0.